Journal of Applied Polymer Science

Crystallization behavior of poly(ethylene terephthalate-*co*-neopentyl terephthalate-*co*-ethylene isophthalate-*co*-neopentyl isophthalate) copolyester and its application in laminated tin-free steel

Liping Ding,[1] Long Xie,[2] Jianyun Cao,[3] Yongping Bai[1]

[1]School of Chemical Engineering and Technology, Harbin Institute of Technology, Harbin 150001, People's Republic of China
[2]R&D Center of Baoshan Iron & Steel Company, Limited, Shanghai 201900, People's Republic of China
[3]Institute for Advanced Ceramics, Harbin Institute of Technology, Harbin, 150001, People's Republic of China
Correspondence to: Y. Bai (E-mail: baifengbai@hit.edu.cn)

ABSTRACT: A low crystallinity, the copolyester poly(ethylene terephthalate-*co*-neopentyl terephthalate-*co*-ethylene isophthalate-*co*-neopentyl isophthalate) (PENIT) was synthesized and applied for laminated tin-free steel. The structures and thermal properties of the copolyester were characterized by ^{1}H-NMR, thermogravimetry analysis, differential scanning calorimetry, wide-angle X-ray diffraction, and polarized optical microscopy. Differential scanning calorimetry, wide-angle X-ray diffraction, and polarized optical microscopy results show that the crystallization ability of the copolyester decreased obviously. Meanwhile, the peel strength, crystallinity, and water-vapor permeability of the copolyester film were also measured at varied lamination temperatures. The result confirm that an improvement in the lamination temperature led to an increased ratio of amorphous PENIT to crystalline PENIT and decreased structural orientation, and the decrease in the structural orientation sped up the increase in the rate of water-vapor permeability. On the basis of the purpose of reducing a detrimental effect on the corrosion resistance caused by water permeation, a reasonable lamination temperature was selected. © 2015 Wiley Periodicals, Inc. J. Appl. Polym. Sci. **2015**, *132*, 42308.

KEYWORDS: polyesters; surfaces and interfaces; synthesis and processing

Received 8 December 2014; accepted 6 April 2015
DOI: 10.1002/app.42308

INTRODUCTION

Polymer-laminated steel has been applied for replacing conventional-polymer-coated steel in Japan since the 1970s because of its cost savings and environmental friendliness. Bi-axis-oriented poly(ethylene terephthalate) (BOPET) film is often used as a laminating material because of its excellently comprehensive properties, including good mechanical strength, high thermal stability, high transparency, relatively light weight, and low water-vapor permeability.[1–5] However, BOPET film is difficult to laminated on steel because of its relatively high melting temperature (T_m) and rigid molecular chains; this greatly limits the application of BOPET film in the industry of polymer-laminated steel.[6–11] Most research activities have focused on the surface performances of poly(ethylene terephthalate) (PET) films to enhance the surface adhesive properties; these methods include graft polymerization and plasma and corona treatments.[12–16] Little attention has been given to the influence of the structure of PET on laminated steel.[17,18]

In this study, a low-crystallinity copolyester, poly(ethylene terephthalate-*co*-neopentyl terephthalate-*co*-ethylene isophthalate-*co*-neopentyl isophthalate) (PENIT), was synthesized and applied in laminated tin-free steel (TFS) without adhesive by a rational yet easily industrialized synthetic approach. Until now, there has been no report on the synthesis of polyester applied in laminated TFS. The structures and properties of the copolyester were characterized by ^{1}H-NMR, differential scanning calorimetry (DSC), thermogravimetry (TG), wide-angle X-ray diffraction (WAXD), and polarized optical microscopy (POM) tests. Furthermore, the effect of the lamination temperature on the properties of the laminated polyester film, including the peel strength, crystallinity, and water-vapor permeability, were investigated carefully. In addition, on the basis of the purpose of reducing the detrimental effect on the corrosion resistance caused by water permeation, a reasonable lamination temperature was selected. Therefore, providing new materials and understanding the changes in the material properties in the lamination process are important and could provide guidance for the development of the PET industry in both theory and practice.

EXPERIMENTAL

Materials

Terephthalic acid (PTA), isophthalic acid (IPA), and ethylene glycol (EG) were purchased from Nuotai Chemicals Fine

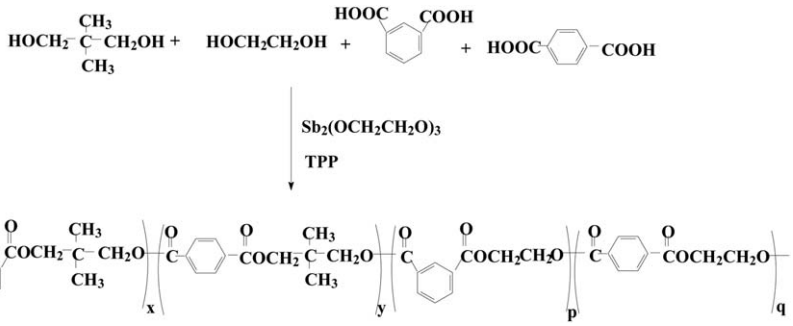

Scheme 1. Synthetic route and structure for the copolyester.

Product Co., Ltd. (Shanghai, China). Neopentyl glycol (NPG) was purchased from Beijing Chemical Reagent Co., Ltd. (Beijing, China). EG antimony was obtained from Shenyang Huachang Antimony Industry Chemical Co., Ltd. Trimethyl phosphate (TPP) was obtained from Tianjing Kermel Chemical Reagents Co., Ltd. (Tianjin, China). TPP was analytical-purity grade, and the rest of chemicals were industrial grade. All of the chemicals were used without further purification.

PET particles and BOPET film as comparison materials were purchased from Shantou Keyi Plastic Co., Ltd. (Shantou, China).

The steel used as the substrate was a TFS supplied by ORG Packaging Co., Ltd. (Shanghai, China). The thickness of steel was 0.176 mm, and the surface of the steel was treated with chromium oxide to increase the adhesion between the TFS and film.

Synthesis of the PENIT Copolyester

The synthetic route for the PENIT copolyester is shown in Scheme 1. The copolyester was prepared via direct esterification and polycondensation in a 5-L stainless steel reactor. The synthetic process was as follows. First, proper amounts of PTA, IPA, EG, NPG [(PTA + IPA)/(EG + NPG) = 1 : 1.4, PTA/IPA = 8 : 1, EG/NPG = 95 : 5 (molar ratio)], ethylene glycol antimony (4/10,000 of total mass), and TPP (1/10,000 of total mass) were added to the reactor. The mixture was stirred for 15 min to mix it thoroughly and then heated to 200°C for 15 min under a nitrogen atmosphere. Consequently, the temperature was increased to 240°C. As soon as the temperature reached 240°C, the esterification step was started, and it was continued until no more water was collected (ca. 3 h). At the end of esterification step, the pressure was reduced to atmospheric pressure. The temperature was then raised to 265°C, and a vacuum was applied to start the polycondensation. The polycondensation was finished when the mechanical stirring power was increased 1.6 times the starting stirring power. The resulting product was obtained as particles after cutting. It is worth mentioning that no solution was used in this reaction; this effectively simplified the preparation processes and purification steps.

Preparation of the Biaxially Oriented Stretching Copolyester Film

The PENIT copolyester was made into a BOPENIT film by Bruckner's biaxially oriented stretching production line (Germany).The film thickness was 20 μm. The parameters of the biaxially oriented stretching production line were as follows: extruder temperature = 250°C, longitudinal tensile temperature = 75°C, stretching ratio = 2.5 : 1, lateral stretching temperature = 96°C, stretching ratio = 3.0 : 1, heat-setting temperature = 105°C, and rewinding speed = 130 m/min.

Lamination of Copolyester Film to Steel

Figure 1 shows the schematic diagram of the lamination method. First the TFS plate was heated to above T_m of the copolyester in a heating chamber to obtain a uniform surface temperature. The heated TFS plate was pressed against the biaxially oriented copolyester film with a roller. The lamination temperature was varied from 225 to 250°C to investigate the effect of the lamination temperature on the properties of the peel strength, crystallinity, and water-vapor permeability of the as-prepared laminated copolyester film. The line speed of steel was 60 m/min, and the roll pressure was 0.05 kg/cm^2. The BOPENIT films with different lamination temperatures were obtained by the dissolution of the steel completely with a 30 vol % hydrochloric acid solution; the remaining BOPENIT films were rinsed with distilled water, dried, and used to measure the DSC and water-vapor permeability.

Intrinsic Viscosity (η) Test

η of the copolyester was measured with a type IC Ubbelohde viscometer (capillary inner diameter =0.8 mm) at 25 ± 0.1°C in phenol and a 1,1,2,2-tetrachloroethane solution (60/40 w/w) at a concentration of 0.5 g/dL. Each value of η was taken as an average of five values on the same sample. The standard deviation each time was smaller than 0.1 s. η is the critical index property of the influence on film forming in the biaxial

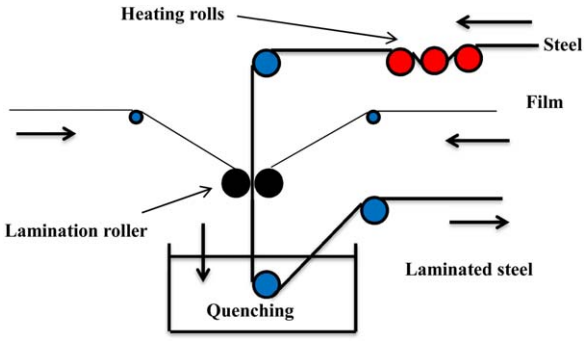

Figure 1. Schematic diagram of the lamination method. [Color figure can be viewed in the online issue, which is available at wileyonlinelibrary.com.]

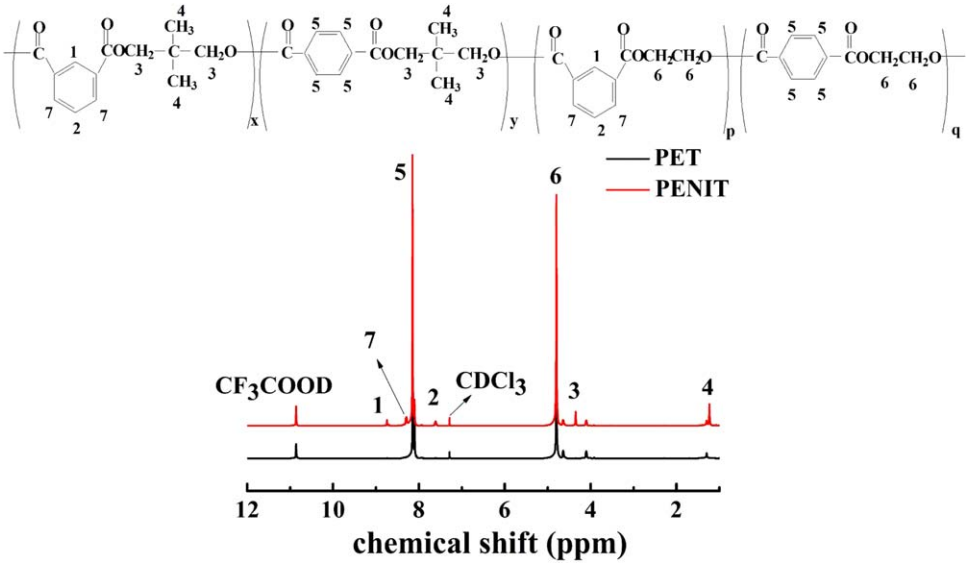

Figure 2. ^{1}H-NMR spectra of the PET and PENIT copolyester. [Color figure can be viewed in the online issue, which is available at wileyonlinelibrary.com.]

stretching process. In the PET industry, to prevent non film formation, η should be between 0.6 and 0.9 dL/g. The calculated PENIT copolyester η was 0.73 dL/g.

^{1}H-NMR Measurement

The ^{1}H-NMR spectra was recorded at room temperature on a Bruker AV-400 spectrometer. Samples were dissolved in $CF_3COOD/CDCl_3$ (1/10 in volume) mixture solvent. The spectrometer was operated at 400 MHz and 25°C with tetramethylsilane as the internal reference with a solution concentration of 0.02 g/mL.

DSC Tests

DSC measurement of the copolyester and PET was carried out on a German NETZSCH 204 instrument with nitrogen as the purge gas. The sample weight was in the range 5–10 mg. We started the experiment by heating each sample from 30 to 300°C at a heating rate of 50°C/min, holding the temperature at 300°C for 3 min to ensure a complete melting of the sample; this was followed by cooling to 30°C at a rate of 10°C/min and then reheating at a ramp rate of 10°C/min to 300°C. The first cooling and the second heating scans were used to determine the melting and crystallization peaks.

DSC measurement of the copolyester films was carried out on the same test equipment in the temperature range from 30 to 300°C at a heating rate of 10°C/min. The heating scans were used to research the crystallinity of the laminated copolyester films.

TG Tests

All TG tests were carried out by a thermal analyzer (PerkinElmer Pyris 1) at a linear heating rate of 10°C/min under a nitrogen atmosphere within the temperature range from 50 to 800°C. The weight of the samples was kept within 2–4 mg.

WAXD Tests

WAXD was used to determine the crystal modification of the biaxially oriented stretched PET and PENIT films. The WAXD intensity pattern of each sample was then collected on a Rigaku X-ray diffractometer equipped with a computerized data collection and analytical toolbox. The X-ray source (Cu Kα radiation $\lambda = 1.54$ Å) was generated with an applied voltage of 40 kV and a filament current of 30 mA. The scan rate was 4° 2θ/min, and the 2θ range was 5–50°. The selected voltage and current were 40 kV and 200 mA, respectively.

POM

The crystallization morphologies of the copolymers were observed with POM (Olympus BX51-P) coupled with a computer-controlled charge-coupled device camera (Olympus, Japan). The isothermal crystallization samples were observed in thin films prepared between microscope coverslips by the melting of the polymer at 300°C for 10 min and then rapidly cooling to the crystallization temperature 210°C for 30 min in a Linkman T95 hot stage. To obtain the nonisothermal crystallization morphologies of the samples, the crystallization process of the samples for POM observation was performed by cooling from the melt to room temperature by air quenching.

Peel Strength Tests

The peel test was carried out according to ASTM B 533-85 standard by a universal tensile machine with a drawing speed of 300 mm/min. The sample length was 100 mm. The force was recorded by the software as a function of the as-measured path. To calculate the peel strength, the maximum value of the recorded force was used and divided by the width of the peeled stripes (25 mm). The average value of five measurements was used in the peel test.

Water-Vapor Permeability

The water-vapor permeability was measured in a round-mouthed cup filled with distilled water. Copolyester films were placed over the top of the cups, and no moisture was lost from the cup except through the copolyester films. The cups were placed in a dryer, and the weight loss was measured after 24 h.

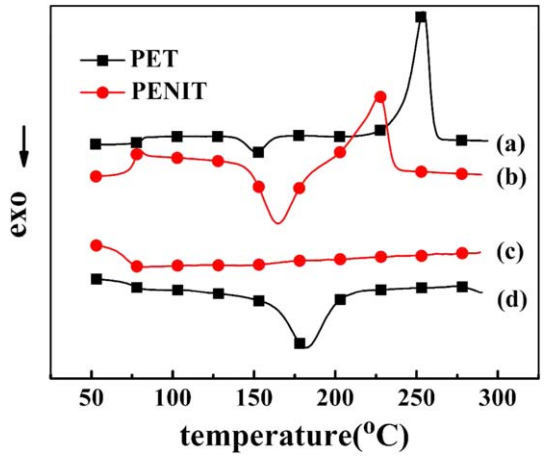

Figure 3. DSC curves of the PET and PENIT copolyester: (a,b) heating process and (c,d) cooling process. [Color figure can be viewed in the online issue, which is available at wileyonlinelibrary.com.]

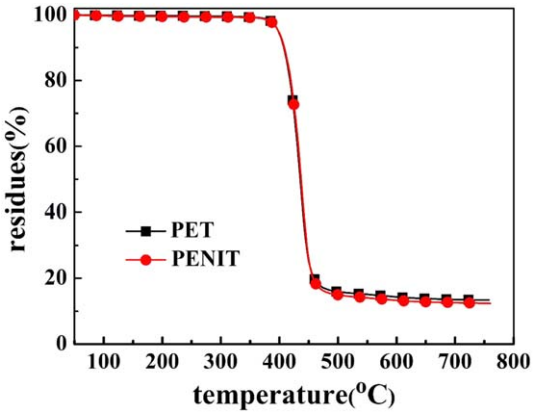

Figure 4. TG curves of the PET and PENIT copolyester. [Color figure can be viewed in the online issue, which is available at wileyonlinelibrary.com.]

The result of water-vapor permeability was calculated with the following equation:[19]

$$\text{Water-vapor permeability} = M/A$$

where M is weight change (mg) and A is the measured area (cm^2). Each value of water-vapor permeability was taken as an average value of five values from the same sample.

RESULTS AND DISCUSSION

^{1}H-NMR Analysis

^{1}H-NMR spectra were used as evidence to confirm the structure of the copolyester. Figure 2 shows the ^{1}H-NMR spectra of the pure PET and PENIT copolyester, in which the possible sequences of PENIT copolyester, and their assignment of proton signals in the PENIT macromolecular chains are also shown. The peaks at 10.86 and 7.28 ppm were associated with the solvent CF_3COOD and $CDCl_3$. Both compounds exhibited intense peaks at 8.14 ppm (peak 5) and 4.79 ppm (peak 6). The peak at 8.14 ppm (peak 5) belonged to the aromatic proton from the PTA unit, and the peak at 4.79 ppm (peak 6) belonged to the —CH_2CH_2— proton from EG unit. In the PENIT copolyester, IPA and NPG were copolymerized with PET. The absorption of the aromatic proton (structural formulas 1, 2, and 7) from the IPA unit occurred at 8.74, 7.59, and 8.31 ppm, respectively. The peaks near 4.3 and 1.2 ppm were the proton absorption of methylene groups (structural formula 3) and methyl groups (structural formula 4) from the NPG unit. The ^{1}H-NMR spectra confirmed the successful synthesis of PENIT copolyester.

DSC Analysis

Figure 3 shows the DSC curves of the PET and PENIT copolyester. Detailed data for the polyester is given in Table I and includes the crystallization temperature in the process of heating (T_{hc}), crystallization temperature in the process of cooling (T_c), and melting temperature (T_m). The melting enthalpy (ΔH_m) and crystallization enthalpy (ΔH_{hc}) were calculated by the corresponding values measured from DSC divided by the weight fraction of the corresponding polyester. The degree of crystallinity (X_c) was calculated from the enthalpy of the second heating process.[20]

Both the heating curves of PET and PENIT copolyester showed crystallization and melting processes. It is worth noting that the values of T_m, ΔH_m, and T_{hc} of PENIT copolyester were all lower when compared with those of PET. For example, during the heating process, the T_m values were 254.2°C for PET and 227.1°C for the PENIT copolyester. ΔH_m of PET was 32.9 J/g; this was higher than the value of 27.7 J/g for the PENIT copolyester. Furthermore, T_{hc} of the PENIT copolyester was 164.8°C; this was higher than the value of PET (151.4°C). This suggested that the inclusion of NPG and IPA monomers improved the crystallization temperature and reduced the crystallization ability of the PET. This was because the NPG molecular structure had two nonpolar methyl substituents to increase the distance between the molecular chains and decrease the regularity of

Table I. Basic Characterizations of the Copolyesters

	TG		DSC							
			Heating						Cooling	
Sample	T_{onset} (°C)	Residue (%)	T_g (°C)	T_{hc} (°C)	T_m (°C)	ΔH_m (J/g)	ΔH_{hc} (J/g)	X_c (%)	T_c (°C)	η (dL/g)
PET	397.5	13.4	81.2	151.4	254.2	32.9	−3.8	23.3	182.1	0.71
PENIT	397.3	12.4	77.6	164.8	227.1	27.7	−23.0	3.7	—	0.73

T_{onset}, the temperature of 5% mass loss measured from TG curves. $X_c = [(\Delta H_m + \Delta H_{hc})/\Delta H_0] \times 100\%$ (where ΔH_0 is the enthalpy of melting of a 100% crystalline form of PET, i.e., 125 J/g).[20]

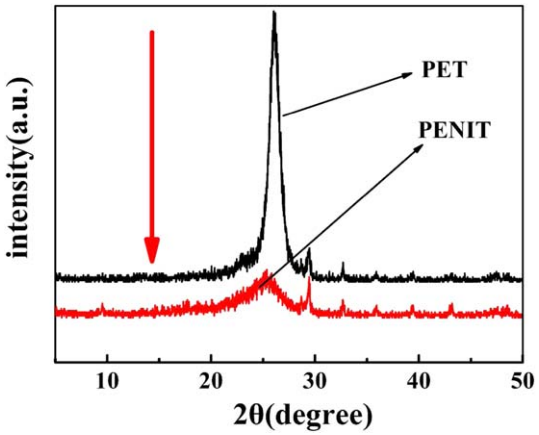

Figure 5. WAXD curves of the biaxially oriented stretching PET and PENIT films at room temperature. [Color figure can be viewed in the online issue, which is available at wileyonlinelibrary.com.]

chain structure; this made chain packing more difficult. Table I reveals that the glass-transition temperature (T_g) declined by approximately 4°C when NPG and IPA were incorporated. T_g was associated with the rotation of the main chain. The incorporation of other monomers reduced the chain stiffness of the PET backbone, promoted its rotation, and reduced T_g. In addition, the copolyesterization monomers were distributed randomly; this disrupted the crystalline regularity and caused a decline of crystallization. This could also be proven by X_c. The X_c value of the PENIT copolyester was 3.7%; this was much lower than that of PET (23.3%). Particularly, in the same cooling process, the PENIT copolyester did not show any crystallization behavior. This also illustrated that the PENIT copolyester had a lower crystal enthalpy and crystallinity compared with PET.

TG Analysis

TG is the most popular method for characterizing the thermal stability of polymers. The thermal stability of the pure PET and PENIT copolyester were studied by TG; the results are shown in Figure 4 and Table I. The PENIT copolyester had a thermal stability of 5% weight loss at a temperature around 397°C; this was to PET. The residues of the PET and PENIT copolyester at 750°C in a nitrogen atmosphere were 13.4 and 12.4%, respectively. The results confirmed that PENIT copolyester had a similar thermal stability to that of PET. Moreover, the PENIT copolyester was thermally stable within the temperature range used in all of the other measurements.

WAXD Analysis

Figure 5 shows the X-ray diffraction patterns of the biaxially oriented stretching PET and PENIT films. The PET and PENIT films showed similar crystal structures. However, the intensity of the diffraction peak at 26°, which corresponded to the reflection of the (100) plane of the copolyester, decreased significantly compared with the PET film. This indicated that X_c measured from X-ray diffraction decreased with increasing comonomer contents. The results again confirm the NPG and IPA monomers could be introduced to decrease X_c of PET.

POM Analysis

Figure 6(a,b) shows the POM micrographs of the copolymers isothermally crystallized at 210°C for 30 min. As shown in Figure 6, the PET and PENIT copolymers exhibited spherulites when crystallized from the melt. All of the spherulites showed similar sizes, as shown in Figure 6(a,b). This indicated that the

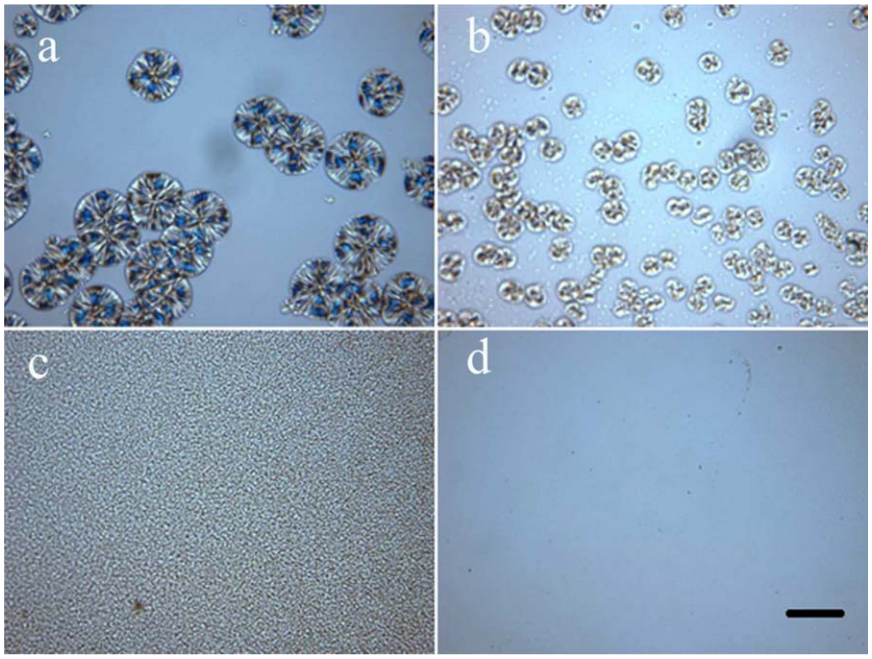

Figure 6. POM images: (a) PET and (b) PENIT copolyester isothermally crystallized at 210°C for 30 min and (c) PET and (d) PENIT copolyester cooled from the melt to room temperature via air quenching. The bar represents 200 μm. [Color figure can be viewed in the online issue, which is available at wileyonlinelibrary.com.]

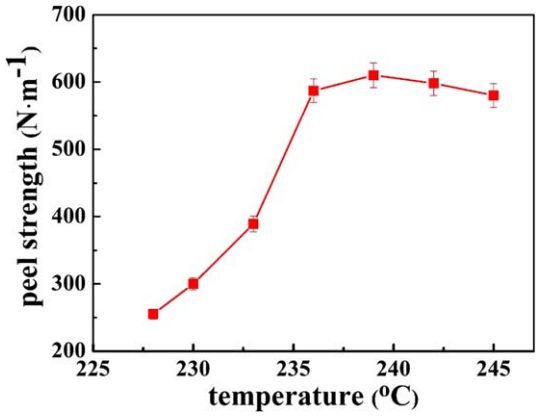

Figure 7. Effect of the lamination temperature on the peel strength of the BOPENIT copolyester film. [Color figure can be viewed in the online issue, which is available at wileyonlinelibrary.com.]

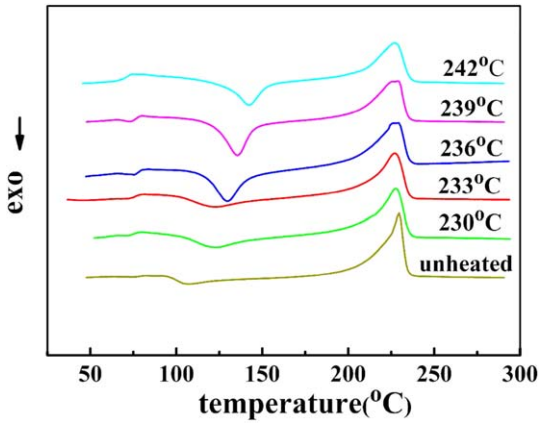

Figure 9. DSC curves of the BOPENIT films with different lamination temperatures. [Color figure can be viewed in the online issue, which is available at wileyonlinelibrary.com.]

nucleation process occurred instantaneously, and the crystal growth was three-dimensional. However, the size of spherulites of PENIT was smaller and more irregular compared with the PET under the same crystal conditions. A similar phenomenon was also observed by Chen *et al.*[21] This meant that for PENIT, it was harder to form a regular spherulite compared with PET. The NPG and IPA monomers decreased the growth rates of the crystals and caused defects in the packing of the crystalline lattices. Until now, there has been little report on the nonisothermal crystallization morphology of PET and its copolymers. However, the study of the nonisothermal crystallization morphology of the copolymers is important because of its link with polymer processing. Figure 6(c,d) shows the crystallization morphologies of copolymers cooling from the melt to room temperature by air quenching. Many tiny crystals were shown in the image of PET [Figure 6(c)], and no crystallization morphology was found in image of PENIT [Figure 6(d)]. This also confirmed that the inclusion of the NPG and IPA monomers decreased the crystallization ability of the PET and made the PET chain packing more difficult.

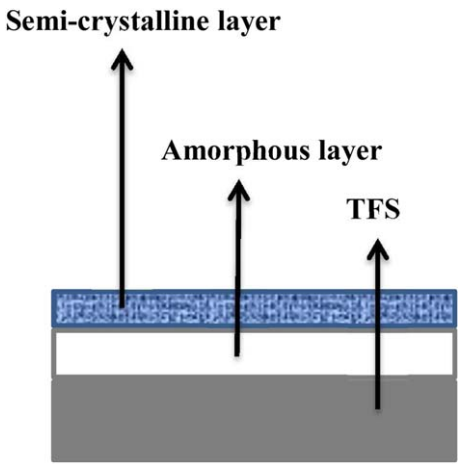

Figure 8. Cross section of the PENIT-film-laminated TFS. [Color figure can be viewed in the online issue, which is available at wileyonlinelibrary.com.]

Effect of the Lamination Temperature on the Peel Strength of the BOPENIT Copolyester Film

The peel strength between the film and substrate is one of the most important properties because the film delamination should be suppressed during the manufacturing process.[22,23] Actually, the substrates are attached by the melting film in the laminating process. So the lamination temperature is a key factor that affects the peel strength of a laminated film. The peel strength of the laminated steels with different lamination temperatures is shown in Figure 7. As shown in Figure 7, the peel strength of the laminated steels increased with increasing lamination temperature. However, the effects of the lamination temperature on the peel strength were obviously different in different temperature ranges. T_m of PENIT was 227.1°C. The film-laminated steel needed to be heated above its T_m and rapidly quenched; a temperature gradient occurred within the film, and a double-layer structure having an inner steel-contacting layer of amorphous PENIT and an outer air-contacting layer of crystal-rich PENIT were formed. This affected the peel strength. The peel strength first increased quickly when the lamination temperature increased from 228 to 236°C and was then stable at a certain value. The reason was that the ratio of amorphous PENIT increased quickly in the temperature range. When the lamination temperature reached 236°C, the BOPENIT film

Table II. DSC Results for the BOPENIT Films

Lamination temperature (°C)	ΔH_{hc}	ΔH_m	Relative X_c (%)
Unheated film	−2.3	25.5	100
230	−6.0	22.9	72.2
233	−5.2	21.9	71.6
236	−14.38	21.4	30.4
239	−14.5	20.6	26.3
242	−14.0	19.84	25.19

X_c is equal to $[(\Delta H_m + \Delta H_{hc})/\Delta H_0] \times 100\%$ (where ΔH_0 is the enthalpy of melting of the unheated BOPENIT copolyester film).

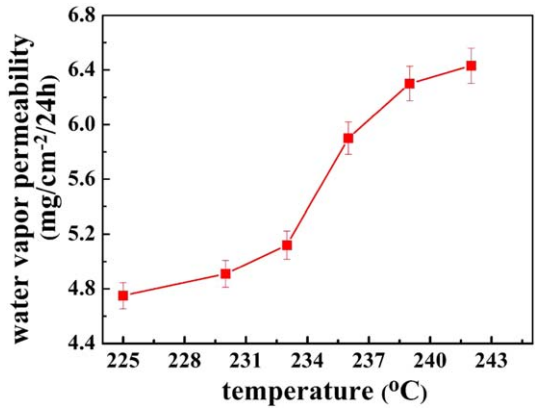

Figure 10. Variation of the water-vapor permeability of the BOPENIT films detached from TFS with various lamination temperatures. [Color figure can be viewed in the online issue, which is available at wileyonlinelibrary.com.]

could not be separated from the steel completely, and the film was split in the lamination area. In contrast, it was difficult to laminate the BOPET film on the steel without the help of adhesives because of its high melting point and rigid structure.

Effect of the Lamination Temperature on the Crystallinity of the BOPENIT Copolyester Film

When the BOPENIT-film-laminated steel was heated to above its T_m and rapidly quenched, an amorphous inner layer was formed, as shown in Figure 8. In the lamination process, the molten BOPENIT film did not have enough time to recrystallize. This was due to the fast cooling and relatively low crystallization rate of PENIT. The ratio of amorphous PENIT to crystalline PENIT was related to the lamination temperature. Figure 9 shows the results of the DSC test of the BOPENIT film with different lamination temperatures. The results are summarized in Table II. ΔH_m and ΔH_{hc} were calculated by the corresponding values measured from DSC divided by the weight fraction of the corresponding polyester film. X_c was calculated from the enthalpy of the heating process.[20] To study the effect of the lamination temperature on the crystallinity of the BOPENIT copolyester film, we assumed that the unheated film was completely crystallized. As shown in Table II, the relative X_c decreased from 72.2 to 26.3% when the lamination temperature was increased from 230 to 250°C. The results demonstrate that the ratio of amorphous PENIT to crystalline PENIT increased with increasing lamination temperature.

Effect of the Lamination Temperature on the Water-Vapor Permeability of the BOPENIT Copolyester Film

The properties of the copolyester film were severely altered in the lamination process because of the change in the crystallinity of the BOPENIT copolyester film, as discussed previously. The water-vapor permeability was an important factor that affects the corrosion at the interface between the BOPENIT film layer and the steel. Figure 10 shows that the water-vapor permeability changed with increasing lamination temperature. As shown in Figure 10, the water permeability improved with increasing lamination temperature. It is worth mentioning that the steep increase of the water-vapor permeability at 233°C was due to the sharp decrease in crystallinity from 71.6 to 30.4% when the lamination temperature increased from 233 to 236°C, as shown in Table II. Nevertheless, Figure 10 shows a continuously growing tendency of the water-vapor permeability curve. The results suggest that the water-vapor permeability of the PENIT copolymer could become larger at a high lamination temperature. As discussed previously, improving the lamination temperature led to an increased ratio of amorphous PENIT to crystalline PENIT and decreased the structural orientation. Meanwhile, the decrease in the structural orientation may have sped up the increase rate of the water-vapor permeability.

On the basis of the analysis of the peel strength and water-vapor permeability, we suggest that the lamination temperature of the laminated steel should not surpass 236°C; this reduced the detrimental effect on the corrosion resistance caused by water permeation in practical application.

CONCLUSIONS

A novel copolyester was synthesized and applied in laminated TFS in this study. The structures and thermal properties of the copolyesters were characterized by ^{1}H-NMR, TG, DSC, and WAXD analysis. The TG results show that the copolyester had a similar thermal stability with PET. However, the DSC, WAXD, and POM results suggested that the inclusion of NPG and IPA monomers reduced the crystallization ability of the copolyester. Meanwhile, the effects of the lamination temperature on the properties of the peel strength, crystallinity, and water-vapor permeability of the copolymer film were thoroughly investigated. The results indicate that with increasing lamination temperature, peel strength, and water permeability also increased. On the basis of the purpose of reducing the detrimental effect on the corrosion resistance caused by the water permeation, the lamination temperature of the laminated steel should not surpass 236°C in practical applications.

REFERENCES

1. Shirali, H.; Rafizadeh, M.; Taromi, F. A. *J. Compos. Mater.* **2014**, *48*, 301.
2. Ding, L.; Bai, Y. *RSC Adv.* **2014**, *4*, 9803.
3. Ding, L.; Shao, L.; Bai, Y. *RSC Adv.* **2014**, *4*, 21782.
4. Pandiyaraj, K. N.; Selvarajan, V.; Deshmukh, R. R.; Bousmina, M. *Surf. Coat. Technol.* **2008**, *202*, 4218.
5. Ke, Z.; Yongping, B. *Mater. Lett.* **2005**, *59*, 3348.
6. De Geyter, N.; Morent, R.; Leys, C. *Nucl. Instrum. Methods Phys. Res. Sect. B* **2008**, *266*, 3086.
7. Pelagade, S. M.; Singh, N. L.; Qureshi, A.; Rane, R. S.; Mukherjee, S.; Deshpande, U. P.; Ganesan, V.; Shripathi, T. *Instrum. Methods Phys. Res. Sect. B* **2012**, *289*, 34.
8. Ding, L.; Wang, L.; Shao, L.; Cao, J.; Bai, Y. *RSC Adv.* **2014**, *4*, 54805.
9. Yang, L.; Chen, J.; Guo, Y.; Zhang, Z. *Appl. Surf. Sci.* **2009**, *255*, 4446.
10. Lu, Y. *Appl. Surf. Sci.* **2010**, *256*, 3554.
11. Sun, J.; Yao, L.; Gao, Z.; Peng, S.; Wang, C.; Qiu, Y. *Surf. Coat. Technol.* **2010**, *204*, 4101.

12. Lu, Y.; Jiang, S.; Huang, Y. *Synth. Met.* **2010**, *160*, 419.
13. Woodward, I.; Schofield, W. C. E.; Roucoules, V.; Badyal, J. P. S. *Langmuir* **2003**, *19*, 3432.
14. Liu, Z.-M.; Xu, Z.-K.; Wang, J.-Q.; Yang, Q.; Wu, J.; Seta, P. *Eur. Polym. J.* **2003**, *39*, 2291.
15. Denes, F. S.; Manolache, S. *Prog. Polym. Sci.* **2004**, *29*, 815.
16. Han, M. H.; Jegal, J. P.; Park, K. W.; Choi, J. H.; Baik, H. K.; Noh, J. H.; Song, K. M.; Lim, Y. S. *Surf. Coat. Technol.* **2007**, *201*, 4948.
17. Cho, C. K.; Kim, J. D.; Cho, K.; Park, C. E.; Lee, S. W.; Ree, M. *J. Adhes. Sci. Technol.* **2000**, *14*, 1131.
18. Brandrup, J.; Immergut, E. H.; Grulke, E. A.; Abe, A.; Bloch, D. R. Polymer Handbook; Wiley: New York, **1999**; Vol. 5, p 101.
19. Wu, Y.; Wang, A. H.; Zheng, R. R.; Tang, H. Q.; Qi, X. Y.; Ye, B. *Appl. Surf. Sci.* **2014**, *305*, 1.
20. Rwei, S.-P.; Lin, W.-P.; Wang, J.-F. *Colloid Polym. Sci.* **2012**, *290*, 1381.
21. Chen, Z.; Yao, C.; Yang, G. *Polym. Test.* **2012**, *31*, 393.
22. Miller, M.; MacDonald, W. A.; Adam, R. *J. Adhes. Sci. Technol.* **2012**, *26*, 55.
23. Jesdinszki, M.; Struller, C.; Rodler, N.; Blondin, D.; Cassio, V.; Kucukpinar, E.; Langowski, H.-C. *J. Adhes. Sci. Technol.* **2012**, *26*, 2357.